Journal of Power Sources 244 (2013) 2–10

Contents lists available at SciVerse ScienceDirect

Journal of Power Sources

journal homepage: www.elsevier.com/locate/jpowsour

Optimum sizing and optimum energy management of a hybrid energy storage system for lithium battery life improvement

Masoud Masih-Tehrani*, Mohammad-Reza Ha'iri-Yazdi, Vahid Esfahanian, Ali Safaei

School of Mechanical Engineering, College of Engineering, University of Tehran, Iran

HIGHLIGHTS

- A formulation is defined for battery and ultracapacitor combination optimum sizing.
- ESS hybridization causes to reduce ESS cost and fuel consumption, simultaneously.
- The HESS optimum sizing shows strong dependency to the vehicle driving cycle.
- The optimum (dynamic programming) power distribution of HESS increases battery life.
- The method is useful for high energy and power application (HEVs, renewable energy).

ARTICLE INFO

Article history:
Received 5 November 2012
Received in revised form
13 April 2013
Accepted 30 April 2013
Available online 21 May 2013

Keywords:
Hybrid energy storage system
Lithium iron phosphate battery life
Optimum power distribution
Optimum sizing
Series hybrid electric bus

ABSTRACT

In this paper, a formulation is developed for sizing of a Hybrid Energy Storage System (HESS) in different applications. Here, the HESS is a combination of Lithium battery and Ultra-Capacitor (UC), which is useful for many high energy and high power applications such as Hybrid Electric Vehicles (HEVs) and renewable energy. The sizing formulas are based on initial cost and 10-years battery replacement cost which is arranged as an optimization problem. For battery replacement cost, the Lithium battery capacity depletion formulas are studied for a $LiFePO_4$ battery. As a case study, application of HESS in a Series Hybrid Electric Bus (SHEB) is considered. The results show by the addition of UC, the Lithium battery life is improved significantly. Furthermore, the optimum sizing of the HESS is dependent to the SHEB driving cycle. Therefore, considering the power profile of the HESS in its sizing process may reduce HESS cost. This effect is studied in three different cycles of the SHEB. In addition, the formulation is applied to cycle-based optimization of the Power Distribution Control Strategy (PDCS) of the HESS by dynamic programming. The results show the optimum PDCS has better $LiFePO_4$ battery life in comparison with the conventional PDCS.

1. Introduction

The energy storage system (ESS) has a key role in many energy generation systems, such as renewable energies. Specially, the ESS is the main drawback in commercialization of different kinds of electric vehicles (EV) and Hybrid Electric Vehicles (HEV). The ESS is an expensive, heavy, and voluminous component of the EV. The characteristics of the ESS lead to limiting the mileage of the electric vehicle [1]. Moreover, life of the ESS as well as the cost of replacing them, prevent manufacturers from bringing EVs into play, even though their fuel economy reduces their everyday cost considerably [2]. Recently, a rapid evolution of EV has begun, which is driven largely by the development of batteries of large storage capacity and reduced cost [3]. In addition, considerable R&D activities are being performed to improve the ESS performance for different applications in the recent years.

The ESS provides the power and energy demands of the energy generation system. Analyzing the demands of many ESS applications shows that the average power demands are very much lower than the peak power demands which occur in short time periods. For example, the electric vehicles are loaded with large peak-to-average power ratios (between 4 and 7) [4]. The most common

Abbreviations: DoD, Depth of Discharge; EV, electric vehicle; ESS, energy storage system; GA, genetic algorithm; HEV, Hybrid Electric Vehicle; HESS, hybrid energy storage system; ICE, Internal Combustion Engine; PDCS, Power Distribution Control Strategy; SHEB, series hybrid electric bus; SoC, state of charge; UC, ultra-capacitor; USD, United States dollar; VFERI, Vehicle, Fuel, and Environment Research Institute.

* Corresponding author. Tel./fax: +98 21 88020741.
E-mail address: masih@ut.ac.ir (M. Masih-Tehrani).

0378-7753/$ – see front matter © 2013 Elsevier B.V. All rights reserved.
http://dx.doi.org/10.1016/j.jpowsour.2013.04.154

Nomenclature

Ah	Ah-throughput
B	pre-exponential factor
C-rate	ratio of battery current to battery capacity
$\text{Cost}_{\text{HESS}}$	equivalent HESS cost
dt	time step of calculation
FUC	UC capacity
I_{bat}	battery current in each time step (k)
I_{UC}	UC current
LC	life capacity
n_{p}	number of the UC modules in parallel configuration
n_{s}	number of the UC modules in series configuration
P_{bat}	battery power
P_{dem}	vehicle demand power
P_{UC}	UC power
Q_{loss}	percentage of capacity loss
$Q_{\text{loss}-10\text{y}}$	10-years capacity loss
R	gas constant
R_{UC}	UC internal resistance
SoC_{UC}	UC SoC
T	absolute temperature
t_{DC}	driving cycle duration
V_{UC}	UC voltage
VOC_{UC}	UC open circuit voltage

ESS of EVs is a battery. Batteries are preferred in the market due to their low cost and portability [5]. Batteries have high energy and low power specifications for use in EVs (peak-to-average power ratios are between 0.5 and 2 [4]). As battery costs continue to decrease, EVs will become more attractive for a larger pool of customers. However, the life-time for battery advances is uncertain [6]. Another candidate for ESS is an ultra-capacitor (UC). The ultra-capacitors have good life cycle, low energy and high power specifications (peak-to-average power ratios are between 10 and 12 [4]). Also, the cost of ultra-capacitors has been falling significantly during the last decade [7]. As stated, the conventional ESSs have either high energy or high power specifications. Therefore, aimed at satisfying the energy and power requirements of the vehicle simultaneously, the design leads to the oversizing of either of them. This oversized design causes expensive, heavy, and voluminous ESS. The complementary specifications of batteries and ultra-capacitors can be beneficially combined to make a new ESS of EVs that shows high performance with low weight and suitable battery life at a reasonable cost [8]. In recent years, some designs have been proposed to implement this idea for developing a hybrid energy storage system (HESS) with high energy and high power specifications. The main objective of coupling batteries and UCs is to reduce the current stress in the batteries and to improve its life-time [9]. The main drawback of the HESS is its cost. Therefore, the sizing optimization is necessary. But, there is a knowledge gap in the literature for economic evaluation of a HESS during its lifespan.

$LiFePO_4$ (lithium iron phosphate) has been considered as one of most capable candidates for HEV applications because of its excellent chemical, thermal stability and low cost [10]. However, capacity depletion behavior and life modeling for this battery has not been well established. More importantly, there is little insight regarding the aging mechanisms associated with this type of battery [11,12]. Wang et al. [10] evaluated the aging mechanisms of $LiFePO_4$ lithium ion battery cells.

The HESS Power Distribution Control Strategy (PDCS) has a great effect on its behavior [13]. The main target of HESS is to moderate the battery currents by the UC. The common PDCS is the UC based PDCS. The PDCS commands the DC/DC converter to utilize the ultra-capacitor pack to provide the vehicle demanded power as a prior energy storage. The remaining demanded power is generated by the battery pack [14]. Furthermore, some additional features for PDCS are introduced in the literature of the HESS, such as the UC state of charge control [15,16].

The PDCS can be presented as a discrete sequential decision problem. Therefore, a forward Dynamic Programming (DP) algorithm is proposed in this paper as an optimum PDCS for optimizing the lithium battery life. This method is used in some recent research in the field of hybrid vehicles [17,18]. The dynamic programming algorithm is a recursive method for achieving the optimal solution in sequential decision problems [19]. By using the DP algorithm to get the optimal solution for a problem, we can avoid the large amount of time which is consumed in the exhaustive search method. The DP algorithm is presented for the first time by Bellman in 1957 [20]. He has introduced the algorithm through a theorem naming as Optimality Principle. Based on this principle [21]:*An optimal path has this characteristic that the taken decisions from each point in the path to the end are optimum regardless of the initial state of the problem. This property is conditioned on existing of connections between the point and the optimal decisions in the former steps.*

Some research works utilized the charge/discharge cycle counting methods to estimate the battery lifetime [2,22]. The complexity of these methods is that there are a few complete cycles during the real battery working situations in electric and Hybrid Electric Vehicles. Thus, the Depth of Discharge (DoD) of cycles are dissimilar and a correction method should be developed. Generally, batteries discharged at higher currents have lower discharge capacities [23]. The rate at which a battery charges and discharges has a clear effect on the capacity fade within batteries as observed by Ramadass et al. [24]. In this paper, a life model for a $LiFePO_4$ battery cell is formulated. This lithium battery life model is applied for the capacity loss calculation in a driving cycle.

As a case study for HESS application, a series hybrid electric bus (SHEB) is studied in this paper. The SHEB has been designed and fabricated in the University of Tehran, Iran [25]. The SHEB is a series HEV in which all of its propulsion energy is produced by the

Table 1
Specifications of LFP26650P power cell (http://store.peakbattery.com).

Characteristic	Value
Nominal capacity @ C/5 (Ah)	2.6
Average operating voltage @ C/5 (V)	3.2
Internal impedance @ 1 kHz, AC (mΩ)	<9
Weight (g)	80.5±2
Recommended operating conditions	
Continuous discharge (A)	≤10
Pulse Discharge (A) 30 s	26
Charge current (A)	≤2.6
Charge voltage cutoff (V)	3.65
Discharge voltage cutoff (V)	2.50
High operating temp (°C)	60
Low operating temp (°C)	−20
Maximum operating conditions	
Continuous discharge (A)	42
Pulse discharge (A) 30 s	50
Short pulse discharge (A)	150
Charge current (A)	5
Charge voltage cutoff (V)	4.1
Discharge voltage cutoff (V)	2.0

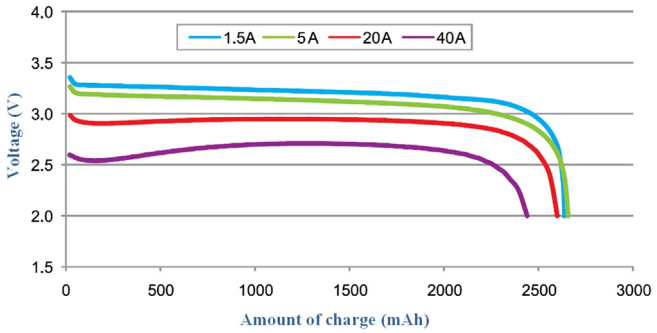

Fig. 1. Voltage curves at different discharge rates for LFP26650P (http://store.peakbattery.com).

electric-machine. Accordingly, the SHEB has high energy and power demands for propulsion.

For the SHEB, the HESS optimum sizing problem is defined and solved by the genetic algorithm in three different driving cycles. Finally, the effects of energy storage hybridization are investigated on the HESS cost and the vehicle fuel consumption.

2. Battery life model

The battery cell of the SHEB is "high capacity LFP26650P power cell" (http://store.peakbattery.com). The specifications of this battery are listed in Table 1. In Fig. 1, the voltage curves at different discharge rates for LFP26650P are presented.

In Fig. 2, the capacity depletion at discharge rate of C/2 as a function of cycle number for different DoD are shown for a $LiFePO_4$ battery cell [10]. The curves of this figure are seen as S-shaped, slightly. This non-linearity shows the complexity of capacity retention during cycle number. Nevertheless, it seems that the linear relation between the capacity retention and cycle number for each DoD is suitable, as a general trend.

The generale life model for all *C*-rates is proposed by Wang et al. [10] in Equation (1).

$$Q_{loss} = B \times \exp((31,700 + 370.3 \times C - \text{rate})/(R \times T))\ (Ah)^{0.55} \quad (1)$$

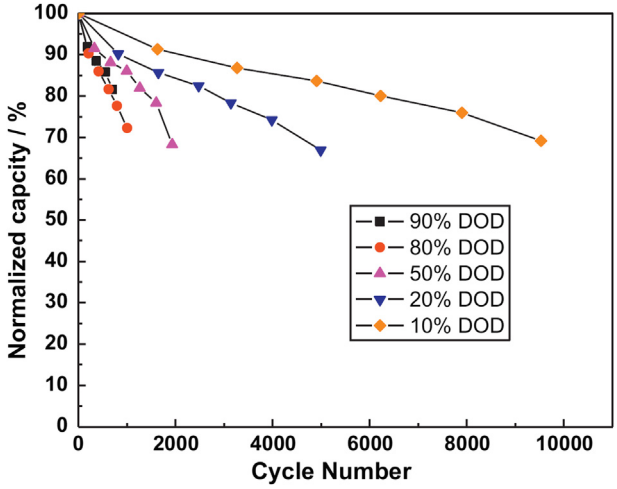

Fig. 2. Capacity depletion at discharge rate of C/2 as a function of cycle number for different DoD [10].

Table 2
Values of *B* respect to *C*-rate.

C-rate	C/2	2C	6C	10C
B values	31,630	21,681	12,934	15,512

which Q_{loss} is the percentage of capacity loss, B is the pre-exponential factor which is dependent on *C*-rate, *C*-rate is the ratio of battery current to battery capacity, R is the gas constant, T is the absolute temperature, and Ah is the Ah-throughput, which is expressed as $Ah = (\text{cycle number}) \times (DoD) \times (\text{full cell capacity})$. The values of B respect to *C*-rate are listed in Table 2.

The life capacity (Ah) of the $LiFePO_4$ battery cell with 2.6 Ah in each battery current are calculated by Equation (1) and listed in Table 3. The life capacity is defined in this paper as the amount of charge that a battery can provide at a specific current before its capacity loss reaches 20%.

In a Hybrid Electric Vehicle, the performances of vehicle are determined in "driving cycles". The driving cycles show the average driving manner in a special situation. There are some standard driving cycles, however, some of them are considered for fuel consumption and emission tests and validation. As shown in Refs. [26], the performances of ESS or HESS are dependent on the aggressiveness of the driving cycle. Therefore, the sizing of a HESS could be done in a specific driving cycle to optimize the equivalent battery cost.

In Equation (2), the driving cycle capacity loss ($Q_{loss-DC}$) is derived.

$$Q_{loss-DC} = \Sigma(I_k \times dt/3600)/(LC(I_k)); \quad k = 0 : t_{DC} \quad (2)$$

which I_k is the battery current in each time step (k) and k varies from zero to the driving cycle duration (t_{DC}). dt is the time step of calculation and LC is the life capacity which is dependent to I_k and is determined using values of Table 3. The 10-years capacity loss ($Q_{loss-10y}$) is shown in Equation (3). In this equation the driving cycle capacity loss is divided by the driving cycle duration and is multiplied by 3600 (converting second to hour), 8 (a day working hours), 250 (a year working days) and 10, for 10-years capacity loss calculation. The duration of 10-years is chosen as a normal lifespan of a vehicle.

$$Q_{loss-10y} = Q_{loss-DC}/t_{DC} \times 3600 \times 8 \times 250 \times 10 \quad (3)$$

Less than one values of $Q_{loss-10y}$ mean that the battery does not need to replacement during 10-years working in a specific driving cycle. If $Q_{loss-10y}$ rounds toward positive infinity ("ceil" function), each ceil ($Q_{loss-10y}$) greater than one shows the quantity of battery replacing during 10-years.

3. Series hybrid electric bus

A series hybrid electric bus has been designed and fabricated in the University of Tehran, Iran. The base vehicle of this SHEB is the

Table 3
Life capacity in different battery current.

Current (A)	Life capacity (Ah)
1	14011
3	11773
5	9641
10	4459
15	1660
20	417

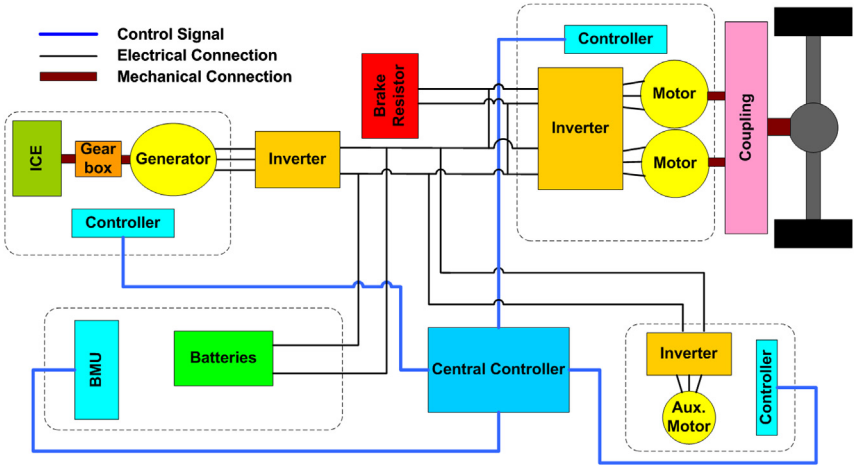

Fig. 3. Series hybrid electric bus powertrain configuration.

O457 city bus. The hybrid powertrain configuration of the O457 SHEB has been presented in Fig. 3.

As shown in Fig. 3, the SHEB powertrain is the series configuration. The propulsion system consists of two traction motors, which are coupled using a coupling gearbox. The use of two AC motors is useful when the bus does not need high power, so one of the motors can be switched off and the efficiency of system increases [27]. The three-phase traction motors can propel and brake the HEB during acceleration and deceleration. The regenerative braking energy can be stored in the batteries. Each three-phase traction motor is driven by an inverter. The inverters are the interfaces between high voltage DC bus and the three-phase traction motors. The high voltage bus of the SHEB is connected to the generator and the batteries. The three-phase generator is connected to the high voltage bus using an inverter. The generator, also, is coupled to the output shaft of the Internal Combustion Engine (ICE) by a gearbox to keep the consistency of their speeds. The ICE-generator can provide average power demands of the SHEB (power follower strategy), or only charge the batteries when they have been depleted (thermostat strategy). These working strategies of the ICE-generator are managed by the hybrid vehicle controller.

The batteries are the main voltage source for the high voltage bus of the SHEB. In the recent past years, Ni-MH is the conventional battery technology for the HEV mass market, which is replaced by lithium-based batteries [28]. One of the well-known rules for series hybrid powertrain design is that the ICE-generator provides the average part and the batteries provide the fluctuation parts of the vehicle power demands. Attending to which strategy (the power follower or the thermostat) has been selected by the hybrid vehicle controller, the power and the energy requirements of the batteries have been determined. The main characteristics of the SHEB are listed in Table 4.

Main specifications of the SHEB powertrain are listed in Table 5.

Table 4
Main characteristics of SHEB.

Characteristic	Value
Vehicle total mass	18000 kg
Rolling resistance coefficient	0.01
Drag coefficient	0.79
Wind speed coefficient	0.2
Frontal area	6.75 m^2
Tire radius	0.508 m

3.1. Series hybrid electric bus model

For the performance evaluation of an under-design vehicle, a proper model is required. Using this model, the ESS or HESS power demands are determined. The ESS candidates are experienced by these power demands. The feed-forward model of hybrid electric bus, which is more appropriate for the powertrain design than the feed-backward models (such as ADVISOR), is developed in MATLAB/Simulink [29] shown in Fig. 4. The causality of a feed-forward model resembles the causality of a real vehicle. The power demand, requested by the driver, gives acceleration and speed. Typical for the feed-forward models, the incorporation of a driver model with the purpose of following a reference speed is given by the driving cycle. This type of model is useful for modeling of the vehicle powertrain dynamic behavior.

In the SHEB model, according to the driving cycle speed, vehicle speed and acceleration, the driver demands a torque by means of acceleration pedal. Then the amount of acceleration pedal will be changed to the driver desired torque (in inverter component) and by use of vehicle speed, the driver demanded power is calculated. The auxiliary load is another part of power that must be supplied. The summation of driver demanded power and auxiliary load is named demanded power (P_{dem}) which is the power that must be supplied to drive vehicle and satisfy the auxiliary demands. The "High Voltage Bus" takes P_{dem} and P_{ICE} (the ICE power) and commands $P_{ESS-dem}$ (the demanded ESS power).

3.2. Series hybrid electric bus control strategy

The main task of the series hybrid electric bus control strategy is to decide how the required power of the traction motors must be distributed between the battery and the ICE-generator. A control

Table 5
Main specifications of SHEB powertrain.

Component	Specification
Nominal high voltage bus	Voltage: 614.4 V Power: 85 kW
Traction motors	Torque: 220 Nm (Peak 530 Nm) Current: 142 A (Peak 300 A)
ICE-generator	Power: 130 kW Current: 200 A
Batteries	15 × 192 LFP26650P power cell Detailed specification in Table 1

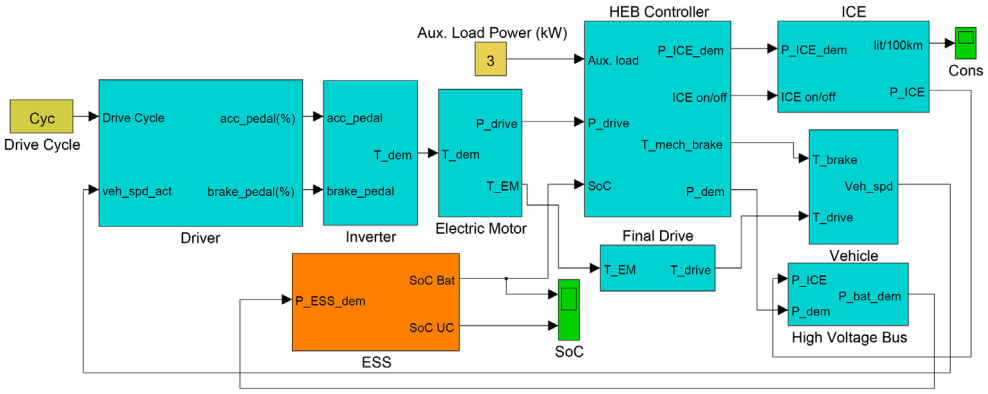

Fig. 4. Feed-forward model of SHEB.

strategy is an algorithm or law for regulating the operation of the drivetrain. It inputs are the measurements of the vehicle operation (e.g., speed, acceleration and grade) and makes decisions to turn on or off certain components or to increase or decrease their power output [30].

In general, power control strategies of series hybrid vehicles can be roughly classified into two kinds: "thermostat" and "power follower" strategies. The thermostat control strategy turns the ICE-generator on and off based on the state of charge (SoC of the batteries). In power follower strategy, the ICE is usually on, and the power output is changed based on the energy requirement.

Manteghi et al. [31] have developed a fuzzy controller as a power follower control strategy for the hybrid electric bus. The fuzzy logic control is chosen because of the need to a controller for a nonlinear, multi-domain and time varying plant with multiple uncertainties.

The main idea of developing a fuzzy controller is to use the advantage of the wide optimal area of the ICE. The controller has been developed to control the engine working point in its optimal region, prevent engine stall due to generator high torque, supply the demanded power by getting the minimum possible use of battery, and maintain the SoC of battery in its efficient region.

The inputs of the fuzzy controller are P_{dem} and SoC and the outputs are ICE on/off and P_{ICE} signals. The fuzzy controller is the "Mamdani" type [32] which takes its input variables, fuzzificate them with the designed membership functions, and then by means of the fuzzy rules the outputs are obtained using the centroid of area method of defuzzification. Outputs of the controller have been simulated and tuned using the feed-forward model. In Fig. 5, a 3-D view of the fuzzy controller is shown.

In the fuzzy controller, the battery usage is less than with the thermostat controller resulting in a longer and safer battery life. In deceleration mode, the fuzzy controller prevents the ICE from producing power so the maximum possible energy is regenerated. On the contrary, in the thermostat controller, sometimes the battery is under charge by the ICE while deceleration happens. Therefore, a large portion of the regenerative power is lost in a brake resistor component. Moreover, the use of the regenerative braking in the thermostat controller is less than with the fuzzy controller [31].

4. Hybrid energy storage optimum sizing

4.1. Driving cycles

The optimum sizing of the HESS of the SHEB is done by evaluation in three different city bus driving cycles. The driving cycles are

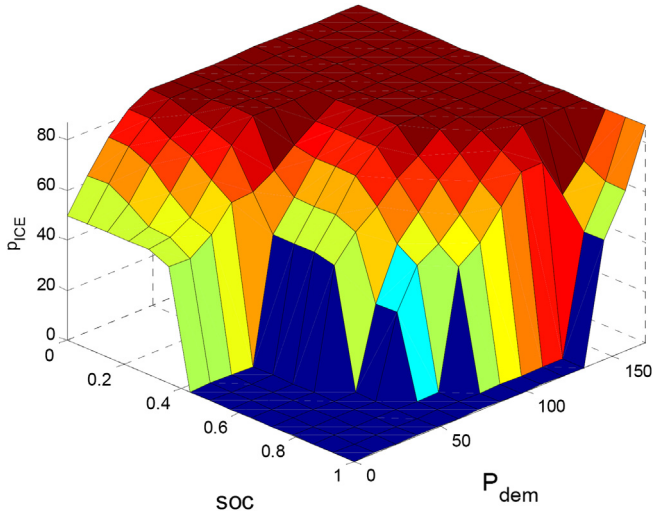

Fig. 5. A 3-D view of the fuzzy controller [31].

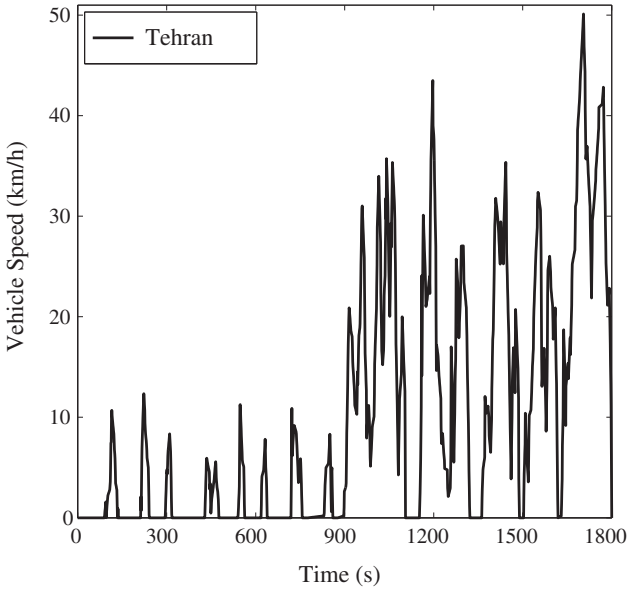

Fig. 6. Tehran city bus driving cycle [33].

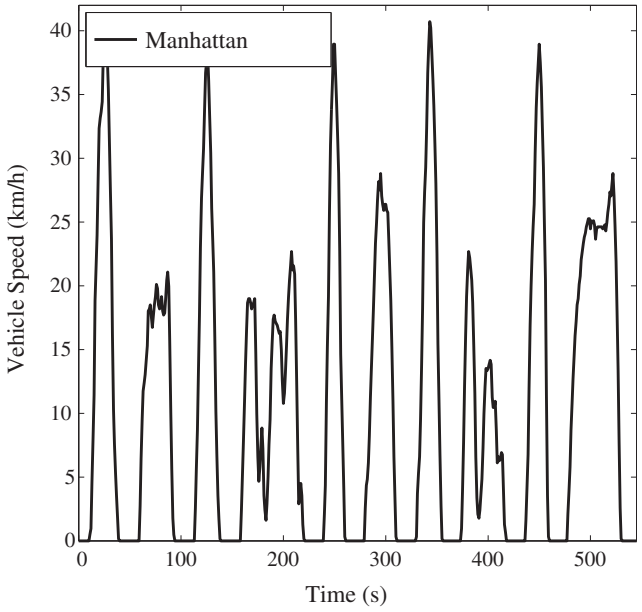

Fig. 7. Manhattan city bus driving cycle (http://www.dieselnet.com).

Tehran (Fig. 6 [33]), Manhattan (Fig. 7 (http://www.dieselnet.com)) and Nuremburg (Fig. 8 (http://www.dieselnet.com)) city bus driving cycles. The driving cycle durations are 1800 s, 545 s and 1081 s, respectively.

4.2. Ultra-capacitor specifications

In Table 6, the ultra-capacitor module characteristics are listed. In comparison with the utilized lithium battery, the power specification of the UC (14.4 kW kg^{-1}) is much higher than of battery (2 kW kg^{-1}) and the energy specification of UC (4 Wh kg^{-1}) is much smaller than of battery (104 Wh kg^{-1}). The power discharge profile of the UC is shown in Fig. 9.

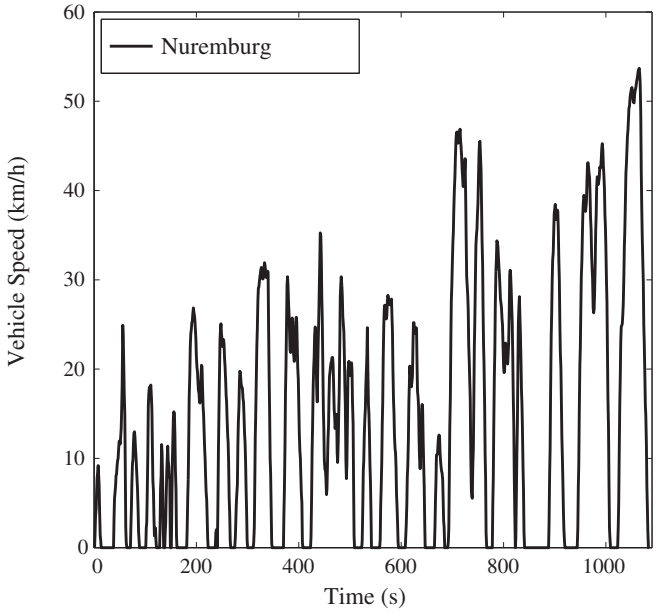

Fig. 8. Nuremburg city bus driving cycle (http://www.dieselnet.com).

Table 6
Ultra-capacitor module characteristics.

Capacitance (F)	Peak current (A)/ Power (kW)(1 s)	Maximum continuous Current (A)/Power (kW)
165	4000/194.4	150/7.3
Nominal voltage (v)	Energy (Wh)	Weight (kg)
48.6	54	13.5

4.3. UC based Power Distribution Control Strategy

The UC based PDCS flowchart is shown in Fig. 10. As a principle rule, P_UC = P_dem (P_UC is the UC power). But, the P_UC is limited by the P_UC_min (the minimum level of the UC power) and the P_UC_max (the maximum level of the UC power). The excess power of the HESS demanded power which the UC cannot provide (P_dem−P_UC) is generated by the battery (P_bat). Likewise, the P_bat is limited by the P_bat_min (the minimum level of the battery power) and the P_bat_max (the maximum level of the battery power).

In Fig. 11, the UC based PDCS behavior examples ((a) during charge and (b) during discharge) are shown. These results belong to the SHEB in Tehran driving cycle. These illustrations present that the UC based PDCS using the UC as a prior ESS. However, when the P_UC is not enough for providing the all of the P_dem, the battery generates the remaining demand power.

4.4. Cost of energy storage components and optimum sizing

In this paper, the cost of energy storage devices are supposed as 1,500–1,800 kWh^{-1} for the LFP26650P power cell battery (http://store.peakbattery.com), 15,000 $ kW h^{-1} for the UC ([34,35]), and 50 USD kW^{-1} for the DC/DC converter [16]. Therefore, the equivalent HESS cost ($Cost_{HESS}$) is determined from Equation (4).

$$Cost_{HESS} = \text{ceil}\left(Q_{loss-10y}\right) \times 40,000 + n_s \times n_p(0.054 \times 15,000 + 7.3 \times 50) \quad (4)$$

which ceil ($Q_{loss-10y}$) is calculated from Equation (3) for each driving cycle, 40,000 USD is the battery pack cost, n_s and n_p are the number of the UC modules in series and parallel configuration for the designed UC pack, respectively. The values of 0.054 kWh, 15,000 USD, 7.3 kW and 50 USD are one-to-one the UC energy capacity, the UC module cost, the UC module power and the DC/DC converter cost. The HESS cost is determined as USD from Equation (4).

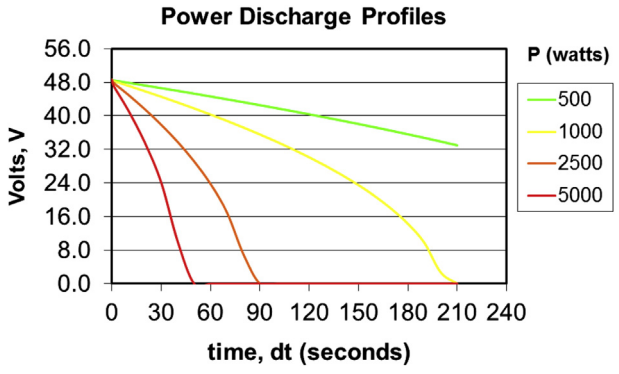

Fig. 9. Power discharge profile of the ultra-capacitor.

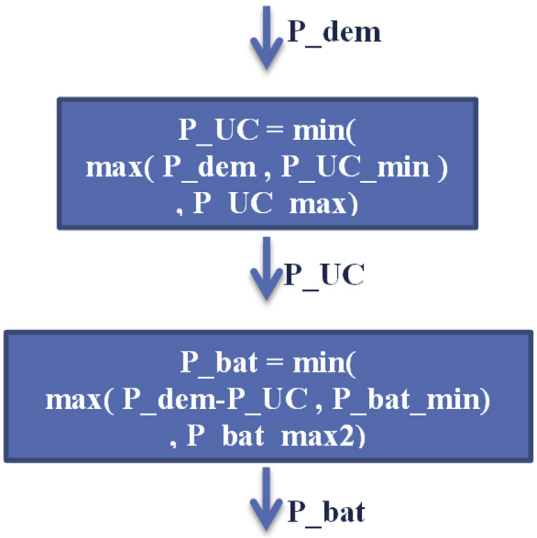

Fig. 10. UC based PDCS flowchart.

Equation (4) is the cost function of the HESS optimum sizing problem. The optimization variables are n_s and n_p, which are integer with feasible intervals [1 ~ 20] and [0 ~ 5], respectively. When $n_p = 0$, there is no UC in the HESS, the energy storage of the SHEB contains only the battery pack.

The strong non-linearity of the cost function of the HESS sizing problem lead to use the heuristic optimization methods. The Genetic Algorithm (GA) optimization method as a well-known and powerful method is selected in this paper.

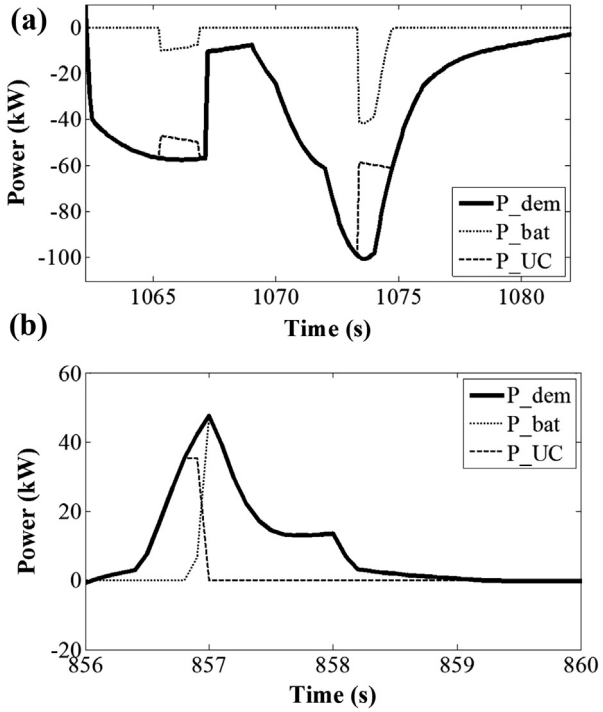

Fig. 11. UC based PDCS behavior examples: (a) during charge (b) during discharge.

Table 7
Main parameters of the DP.

Parameter	Value
Time step	1 s
SoC discretization step	0.5%
Initial battery SoC	70%
Initial and final UC SoC	90%
Minimum UC SoC	20%
Maximum UC SoC	100%

5. Optimum Power Distribution Control Strategy

The dynamic programming is used as the optimum PDCS of HESS. Main parameters of the DP are listed in Table 7.

The discretized solution space for performing the DP algorithm is shown in Fig. 12.

The power and current of the UC in each time step ($P_{UC,k}$ and $I_{UC,k}$) are calculated from the UC SoC values in the previous and present time steps ($SoC_{UC,k-1}$ and $SoC_{UC,k}$) (Equation (5)).

$$\begin{aligned} I_{UC,k} &= F_{UC} \times VOC_{UC,\max} \frac{SoC_{UC,k-1} - SoC_{UC,k}}{t_s \times 100} \\ V_{UC-t,k} &= VOC_{UC,k} - I_{UC,k} \times R_{UC} \\ P_{UC,k} &= I_{UC,k} \times V_{UC-t,k} \end{aligned} \tag{5}$$

which F_{UC} is the UC capacity (F), $VOC_{UC,\max}$ is the maximum open circuit voltage of the UC, $V_{UC-t,k}$ is the UC voltage in k step time, $VOC_{UC,k}$ is the open circuit voltage of the UC in k step time, and R_{UC} is the UC internal resistance.

The battery power ($P_{bat,k}$) is determined in Equation (6) from the vehicle demand and UC powers ($P_{dem,k}$ and $P_{UC,k}$) in each step time.

$$P_{bat,k} = P_{dem,k} - P_{UC,k} \tag{6}$$

The cost function for finding the optimum path (P_{UC} and P_{bat} signals in a driving cycle) is considered Q_{loss} (Equation (1)). In Fig. 13 the process to find the optimal decision in each time step [17] is presented.

In Fig. 14, the optimum PDCS behavior examples ((a) during charge (b) during discharge) are shown. These results belong to the SHEB in Nuremberg driving cycle. As shown in this figure, some behaviors of the optimum are similar to the UC based PDCS (domains 1, 3 and 5 during charge (a) and all domains during discharge (b)). In domains 2 and 4 during charge, when the UC is reached to its limits, the optimum PDCS discharges the UC to prepare it for

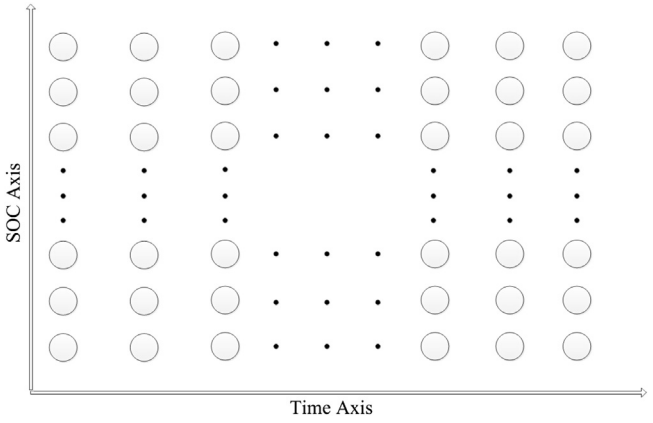

Fig. 12. The discretized solution space for performing the forward DP algorithm.

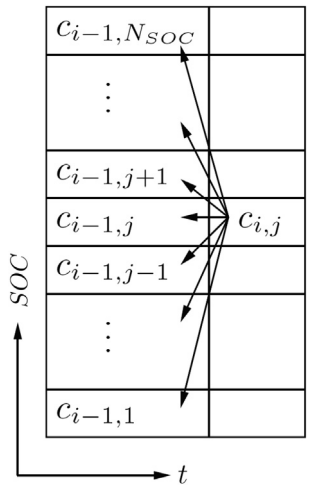

Fig. 13. The process to find the optimal decision in each time step [17].

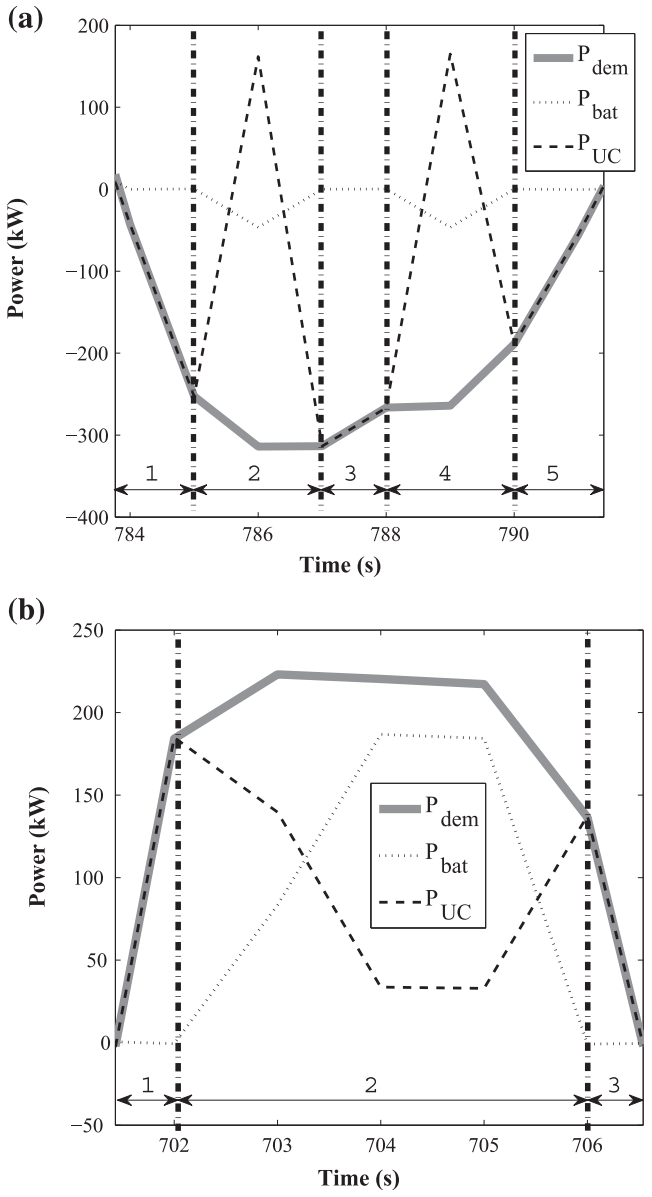

Fig. 14. Optimum PDCS behavior examples: (a) during charge (b) during discharge.

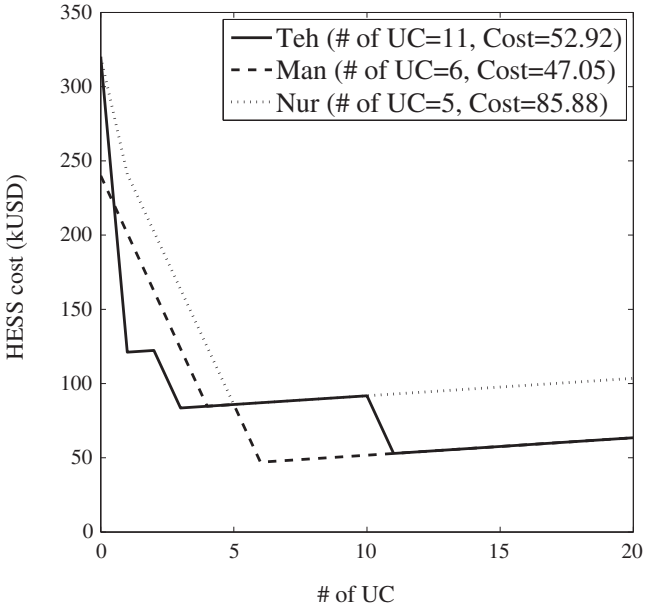

Fig. 15. HESS optimum sizing in different driving cycles.

absorbing more charges. This behavior of the optimum PDCS is exclusive.

6. Results

In Fig. 15, HESS optimum sizing in different driving cycles are presented. These curves are determined by GA. The solid line is for Tehran, the dashed line is for Manhattan and the dotted line is for Nuremburg. As shown in this figure, the battery initial and replacement costs for ESS are about 250 kUSD and higher. The HESS costs are between four times to five times lower than ESS cost, due to less battery replacement needs in 10-years.

The effects of ESS hybridization are listed in Table 8. The results of ESS hybridization show the significant improvement in ESS 10-years cost (at least 73%) and vehicle fuel consumption (at least 26%). Therefore, UC addition in conventional ESS causes to reduce battery replacement needs in 10-years lifespan of an electric vehicle. Furthermore, the reduction of fuel cost is another advantage of ESS hybridization. As seen in Table 8, the optimum number of UC and the effects of ESS hybridization are varied in different driving cycles. Consequently, for a city bus with an approximately specific driving cycle in whole of its working days, the driving cycle-based optimization is necessary (Table 9).

In Fig. 16, Optimum and UC based PDCSs comparison is presented in a section of Nuremburg driving cycle. The solid line is for ESS, the dotted line with circles is for dynamic programming (optimum PDCS) and the dashed line with trapezoids is for UC based PDCS. As shown in these curves, the UC based Q_{loss} is lower than ESS ones, significantly. However, the optimum PDCS Q_{loss} is better than UC based PDCS ones.

Table 8
Effects of ESS hybridization.

Performances	Tehran	Manhattan	Nuremburg
# of UC	11	6	5
Cost improvement (%)	83.46	80.40	73.16
Fuel consumption improvement (%)	41.74	29.68	26.85

Table 9
Optimum and UC based PDCSs comparison.

	ESS	Optimum PDCS	UC based PDCS
$Q_{loss}(10^{-3})$	4.59	0.62	0.88
% Improvement	–	86.53	80.74

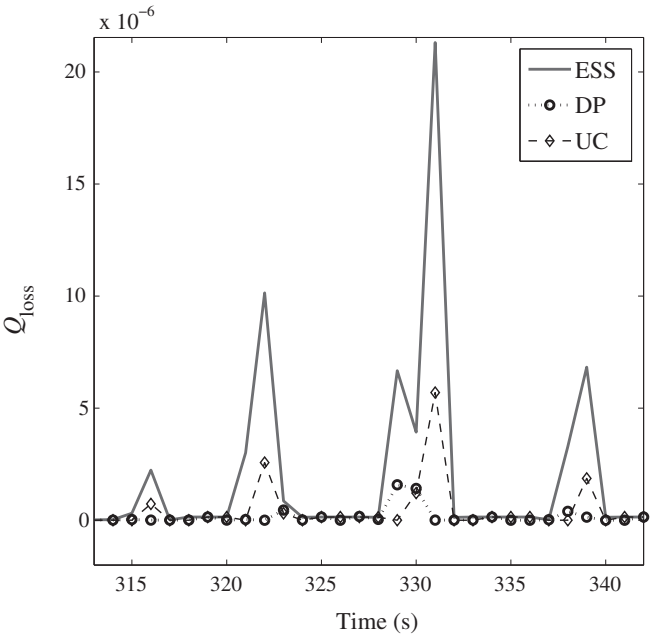

Fig. 16. Q_{loss} comparison.

7. Conclusion

A formulation was defined for energy storage hybridization sizing. In this paper, the HESS is a combination of lithium battery and UC, which is useful for many high energy and high power applications such as HEVs and renewable energy. The formulas were developed as an optimization problem respect to working profile of the HESS. The cost function consists of the initial battery cost and the 10-years battery replacement costs for a $LiFePO_4$ battery. As a case study, application of HESS in a series hybrid electric bus (SHEB) was studied. The results showed that energy storage hybridization causes to reduce the ESS cost and the vehicle fuel consumption, simultaneously. In addition, the HESS optimum sizing shows strong dependency to the working profile. Therefore, considering the power profile of the HESS in its sizing process may reduce HESS cost. In addition, the formulation was applied to cycle-based optimization of the Power Distribution Control Strategy (PDCS). The dynamic programming method was used to optimize the Power Distribution Control Strategy. The optimum PDCS increased the $LiFePO_4$ life in comparison with the conventional PDCS. The proposed algorithm is suitable to optimize the HESS sizing and its PDCS for extensive range of HESS applications.

Acknowledgment

This work was supported by the University of Tehran and Vehicle, Fuel and Environment Research Institute (VFERI) of University of Tehran, Iran.

References

[1] M. Ye, Z. Bai, B. Cao, Journal of Automobile Engineering 222 (2008) 1827–1839.
[2] M. Amiri, M. Esfahanian, M. Hairi-Yazdi, V. Esfahanian, Journal of Power Sources 190 (2009) 372–379.
[3] W. Liu, J. Drobnik, European Electric Vehicle Congress (EEVC), 2011.
[4] R. Schupbach, J. Balda, M. Zolot, B. Krmer, in: IEEE Power Electronics Specialists Conference, PESC03 (2003).
[5] S. Lukic, J. Cao, R. Bansal, F. Rodriguez, A. Emadi, IEEE Transactions on Industrial Electronics 55 (2008) 2258–2267.
[6] W. Sierzchula, S. Bakker, K. Maat, B. Wee, European Electric Vehicle Congress (EEVC), 2011.
[7] M. Leiber, Vehicle Electrification (2011).
[8] P. Bubna, S. Advani, A. Prasad, Journal of Power Sources 199 (2012) 360–366.
[9] A. Allegre, A. Bouscayro, R. Trigui VPPC'09, in: Vehicle Power and Propulsion Conference, IEEE, 2009.
[10] J. Wang, P. Liu, J. Hicks-Garner, E. Sherman, S. Soukiazian, M. Verbrugge, H. Tataria, J. Musser, P. Finamore, Journal of Power Sources 196 (2011) 3942–3948.
[11] Y. Hu, H. Liu, International Journal of Digital Content Technology and Its Applications 6 (2012) 264–272.
[12] A. Guerfi, Y. Dontigny, M. Kobayashi, A. Vijh, K. Zaghib, Journal of Solid State Electrochemistry 13 (2009) 1003–1014.
[13] A. Burke, International Journal of Energy Resources 34 (2010) 133151.
[14] Z. Amjadi, S.S. Williamson, IEEE Transactions on Industrial Electronics 57 (2010) 608–616.
[15] H. Yoo, S.-K. Sul, Y. Park, J. Jeong, IEEE Transactions on Industry Applications 44 (2008) 108–114.
[16] J. Dixon, I. Nakashima, E. Arcos, M. Ortzar, IEEE Transactions on Industrial Electronics 57 (2010) 943–949.
[17] H. Wegleiter, G. Schweighofer, B. Holler, R. Brunnader, European Electric Vehicle Congress (EEVC), 2011.
[18] A. Safaei, V. Esfahanian, M.-R. Hairi-Yazdi, M. Esfahanian, M. Masih-Tehrani, H. Nehzati, in: Article of the ASME 2012 11th Biennial Conference on Engineering Systems Design and Analysis (ESDA2012), 2012.
[19] J. Seinfeld, L. Lapidus, Industrial and Engineering Chemistry Process Design and Development 7 (1986) 475–478.
[20] R. Bellman, Dynamic Programming, Princeton University Press, Princeton, N. J., 1957.
[21] D. Kirk, Optimal Control Theory, An Introduction, Dover Publications, Inc., 1970.
[22] E. Schaltz, A. Khaligh, P. Rasmussen, IEEE Transactions on Vehicular Technology 58 (2009) 3882–3891.
[23] J. Kowski, Advances in Lithium Ion Batteries Obviate Need for Ultracapacitors in Electric Vehicles (2010). Ph.D. thesis.
[24] P. Ramadass, B. Haran, R. White, B.N. Popov, Journal of Power Sources 112 (2002) 614–620.
[25] F. Sangtarash, V. Esfahanian, H. Nehzati, S. Haddadi, M. Amiri, B. Haghpanah, SAE International Journal of Fuels and Lubricants 1 (2009) 828–837.
[26] M. Masih-Tehrani, D. Bazargan, M. Hairi-Yazdi, M. Esfahanian, in: Power Electronics, Drive Systems and Technologies Conference (PEDSTC), 2011.
[27] M. Esfahanian, V. Esfahanian, F. Sangtarash, M. Amiri, A. Khanipour, The FISITA 2006 World Automotive Congress, 2006.
[28] J. Wiaux, European Electric Vehicle Congress (EEVC), 2011.
[29] V. Esfahanian, H. Nehzati, M. Masih-Tehrani, A. Safaei, in: The International Conference on Powertrain Modelling and Control (PMC 2012), 2012.
[30] M. Ehsani, Y. Gao, A. Emadi, Modern Electric, Hybrid Electric, and Fuel Cell Vehicles: Fundamentals, Theory and Design, CRC Press, 2009.
[31] A. Manteghi, V. Esfahanian, M. Amiri, H. Nehzati, The FISITA 2008 World Automotive Congress, 2008.
[32] L.X. Wang, A Course in Fuzzy Systems and Control, Prentice-Hall International, Inc., New Jersey, USA, 1997.
[33] M. Montazeri-Gh, H. Varasteh, M. Naghizadeh, in: Powertrain & Fluid Systems Conference & Exhibition, 2005.
[34] R. Doucette, M. McCulloch, Journal of Power Sources 196 (2011) 1163–1170.
[35] Q. Caia, D. Bretta, D. Browningb, N. Brandon, Journal of Power Sources 195 (2010) 6559–6569.